ISSN 1560-3547, Regular and Chaotic Dynamics, 2013, Vol. 18, No. 5, pp. 521–538. © Pleiades Publishing, Ltd., 2013.

# Richness of Chaotic Dynamics in Nonholonomic Models of a Celtic Stone

**Alexander S. Gonchenko[1*], Sergey V. Gonchenko[1**], and Alexey O. Kazakov[1,2***]**

[1] *Research Institute of Applied Mathematics and Cybernetics, Nizhny Novgorod State University, ul. Ul'yanova 10, Nizhny Novgorod, 603005 Russia*

[2] *Institute of Computer Science, ul. Universitetskaya 1, Izhevsk, 426034 Russia*

Received June 25, 2013; accepted September 12, 2013

**Abstract**—We study the regular and chaotic dynamics of two nonholonomic models of a Celtic stone. We show that in the first model (the so-called BM-model of a Celtic stone) the chaotic dynamics arises sharply, during a subcritical period doubling bifurcation of a stable limit cycle, and undergoes certain stages of development under the change of a parameter including the appearance of spiral (Shilnikov-like) strange attractors and mixed dynamics. For the second model, we prove (numerically) the existence of Lorenz-like attractors (we call them discrete Lorenz attractors) and trace both scenarios of development and break-down of these attractors.

MSC2010 numbers: 37J60, 37N15, 37G35

**DOI:** 10.1134/S1560354713050055

Keywords: celtic stone, nonholonomic model, strange attractor, discrete Lorenz attractor, Shilnikov-like spiral attractor, mixed dynamics

## 1. INTRODUCTION

In this paper we study the dynamics of the nonholonomic model of a Celtic stone (also called "rattleback", "celt" etc.) moving on a plane. It is well known that such a model allows one to answer the main question of Celtic stone dynamics — the nature of reverse, i.e., rotational asymmetry, which results in the fact that the stone can rotate freely in one direction (e.g. clockwise) but "does not want" to rotate in the opposite direction (counterclockwise). In the latter case it performs several rotations due to inertia, then stops rotating and starts oscillating, after that it changes the direction of rotation and finally continues rotating freely (clockwise).

A mathematical explanation of this phenomenon seems now simple enough. Like most of the well-known nonholonomic mechanical models, the Celtic stone model is described by a reversible system, i.e., a system that is invariant with respect to the coordinate and time change of the form $X \to \mathcal{R}\, X,\ \ t \to -t$, where $\mathcal{R}$ is an involution — a specific diffeomorphism of the phase space such that $\mathcal{R}^2 = Id$. However, in the case of a Celtic stone, this system is, in general, neither conservative nor integrable, although it possesses two independent integrals. Because of this, the system can possess, on a common level set of the integrals, asymptotic stable and completely unstable solutions, stationary (equilibria), periodic (limit cycles) solutions etc., $\mathcal{R}$-symmetric with respect to each other. Then, for example, a stable equilibrium corresponds to a stable vertical rotation of the stone, and an unstable equilibrium symmetric with respect to it corresponds to an unstable rotation in the opposite direction. Such an explanation of the reverse in Celtic stone

*E-mail: agonchenko@mail.ru
**E-mail: gonchenko@pochta.ru
***E-mail: kazakovdz@yandex.ru

dynamics was given in a series of papers: by I. S. Astapov [1], A. V. Karapetyan [2], A. P. Markeev [3] and others (further references can be found in [4], Section 3.6).

Nevertheless, the motion of a Celtic stone is still regarded in mechanics as one of the most complicated and poorly studied types of rigid body motion. Moreover, this is one of the few types of motion in which chaotic dynamics was observed. Recently complex chaotic dynamics has also been found in a model featuring an unbalanced rubber ball (a dynamically asymmetric ball with a displaced center of gravity) moving on a plane, see [5, 6].

Strange attractors in Celtic stone dynamics were first found by A. V. Borisov and I. S. Mamaev [7, 8]. In the present paper we continue these investigations. However, our point of view differs from that of [7, 8]: as it seems to us, the chaotic dynamics associates here not only with strange attractors (SA). Although they exist for some values of parameters (for example, we have a numerical evidence on the existence of Shilnikov-like spiral attractors [9]), it is very interesting that a new kind of dynamical chaos can be observed here — the so-called *mixed dynamics* [10–13]. In this case the set of nonwandering orbits of the corresponding system possesses the following properties:

- it contains hyperbolic periodic orbits of all possible topological types, i.e., stable, completely unstable, saddle-type and, since the system is reversible, symmetric elliptic periodic orbits;
- the closures of the sets of periodic orbits of different types have non-empty intersections.

These properties imply that "attractors" and "repellers" (here $\omega$- and $\alpha$-limit sets of a system) have a non-empty intersection.

**Remark 1.** This intersection itself can be very complicated. An attractor belonging to a Newhouse region[1)] in which systems with infinitely many periodic sinks and sources are dense may serve as a mathematical image of mixed dynamics. As follows from [18] (an analogous argumentation is also contained in [19]), for such Newhouse regions it is generic[2)] that the $\alpha$- and $\omega$-limit sets of a system contain in the intersection a "horseshoe" — some nontrivial uniformly hyperbolic set. Note that Newhouse regions with mixed dynamics exist, for example, near two-dimensional diffeomorphisms having nontransversal heteroclinic cycles (contours) containing fixed saddle points with the Jacobians $> 1$ and $< 1$, [10]. The existence of such regions in the space of two-dimensional reversible diffeomorphisms was proved in [12, 13]. This result must also hold for higher dimensions.

In the present paper we study chaotic dynamics in two different Celtic stone models using both qualitative and numerical methods. These models are described by the six-dimensional system of differential equations (see Section 2). The numerical experiments were performed using the software package "Chaos" developed at the Institute of Computer Science, Udmurt State University, Izhevsk, Russia.

The first model (see Section 2 (2.1)-(2.5)) deals with a stone having physical and geometrical parameters given by (3.1); we call it *BM-stone*, since its chaotic dynamics was first studied by Borisov and Mamaev [7, 8]. In Section 3 we show new results on the chaotic dynamics of the BM-stone. We trace the stages of development of chaotic dynamics in the BM-stone: the onset of chaos; qualitative changes in its structure, including the birth of a spiral attractor (when the limit set contains a saddle focus with negative divergence), and mixed dynamics — a spiral attractor-repeller (when the limit set contains both saddle foci symmetric with respect to each other); the appearance of the elements of conservative dynamics.

The second stone, with the parameters (4.1), is interesting primarily in that *Lorenz-like attractors for diffeomorphisms* (we also call them *discrete Lorenz attractors*) are observed in its nonholonomic model. Accordingly, we study this phenomenon in Section 4. Recall that the discrete Lorenz attractor is a strange attractor with the following properties:

[1)] Recall that *Newhouse regions* are called open (in $C^r$-topology, $r \geqslant 2$) domains from the space of dynamical systems in which systems with homoclinic tangencies are dense. S. Newhouse [14] has proved that such regions exist in any neighborhood of any two-dimensional diffeomorphism with homoclinic tangency. This result was extended to the multidimensional case in [15–17].

[2)] A property is said to be *generic* if it is valid for a residual (of the second Baire category) subset of some open set (this subset is obtained as an intersection of a countable collection open and dense subsets).

1) it looks like the famous attractor from the Lorenz model (compare Figs. 6a and 6b), in particular, the discrete Lorenz attractor has one fixed point, a saddle for which the unstable invariant manifolds form a "homoclinic butterfly";
2) it possesses the so-called pseudo-hyperbolic structure, like the Lorenz attractor, i.e., there exist invariant directions along which the map is strongly contracting, while the map expands volumes in transverse directions (see the exact definition 1).

Thus, the discrete Lorenz attractor is a genuine SA, the same as hyperbolic and Lorenz attractors, since pseudo-hyperbolicity persists for all close systems [20, 21] and it prevents the existence of stable periodic orbits inside the attractor (this is not the case for many SA like the Hénon-like attractors).

Note that discrete Lorenz attractors were first found in three-dimensional Hénon maps [22]. However, as we know, the Celtic stone model is the first model from applications where such interesting and genuine attractors were found [23, 24].

For the reader's convenience, an Appendix containing the main notations related to the discrete Lorenz attractors is presented (see Section 4) .

## 2. EQUATIONS OF MOTION AND THEIR PROPERTIES

We study the dynamics of a rigid body moving on a plane without slipping. This means that we consider a nonholonomic model of motion in which the contact point of the body has zero velocity. The latter implies that $\boldsymbol{v}+\boldsymbol{\omega}\times\boldsymbol{r}=0$, where $\boldsymbol{r}$ is the radius vector from the center of mass $C$ to the contact point, $\boldsymbol{v}$ is the velocity of $C$ and $\boldsymbol{\omega}$ is the angular velocity of the body. As usual, the coordinates of all vectors are defined in some coordinates rigidly attached to the body. Then the equations of motion can be written in the form [25]

$$\begin{aligned}\dot{\boldsymbol{M}} &= \boldsymbol{M}\times\boldsymbol{\omega}+m\dot{\boldsymbol{r}}\times(\boldsymbol{\omega}\times\boldsymbol{r})+mg\boldsymbol{r}\times\boldsymbol{\gamma},\\ \dot{\boldsymbol{\gamma}} &= \boldsymbol{\gamma}\times\boldsymbol{\omega},\end{aligned}\tag{2.1}$$

where $\boldsymbol{M}$ is the angular momentum of the body with respect to the contact point, $\boldsymbol{\gamma}$ is the unit vertical vector and $mg$ is the gravity force. Vectors $\boldsymbol{M}$ and $\boldsymbol{\omega}$ are related by

$$\boldsymbol{M}=[\boldsymbol{I}+m(\boldsymbol{r},\boldsymbol{r})\cdot\boldsymbol{E}-m\boldsymbol{r}\cdot\boldsymbol{r}^T]\cdot\boldsymbol{\omega},\tag{2.2}$$

where where $\boldsymbol{I}$ is the inertia tensor, $\boldsymbol{E}$ is the $3\times 3$ identity matrix and $(\cdot)$ means the matrix product. Equation (2.1) admits two integrals

$$\mathcal{H}=\frac{1}{2}(\boldsymbol{M},\boldsymbol{\omega})-mg(\boldsymbol{r},\boldsymbol{\gamma})\ \text{ and }\ (\boldsymbol{\gamma},\boldsymbol{\gamma})=1,\tag{2.3}$$

*an energy integral* (the first integral) and *a geometric integral*, respectively.

We consider the Celtic stone whose surface $F(\boldsymbol{r})$ has the shape of an *elliptic paraboloid*

$$F(\boldsymbol{r})=\frac{1}{2}\left(\frac{r_1^2}{a_1}+\frac{r_2^2}{a_2}\right)-(r_3+h)=0,$$

where $a_1$ and $a_2$ are the principal radii of curvature at the paraboloid vertex $(0,0,-h)$, and the center of mass is the point $r_1=r_2=r_3=0$. Therefore, the vector $\boldsymbol{r}$ and $\boldsymbol{\gamma}$ are related by:

$$r_1=-a_1\frac{\gamma_1}{\gamma_3},\ \ r_2=-a_2\frac{\gamma_2}{\gamma_3},\ \ r_3=-h+\frac{a_1\gamma_1^2+a_2\gamma_2^2}{2\gamma_3^2}.\tag{2.4}$$

It is also assumed that one of the principal axes of inertia is vertical. One of the main features of the Celtic stone is that two other principal axes of inertia have been rotated about the geometrical axes by some angle $\delta$, where $0<\delta<\pi/2$. Accordingly, the inertia tensor takes the following form [8]:

$$\boldsymbol{I}=\begin{pmatrix} I_1\cos^2\delta+I_2\sin^2\delta & (I_1-I_2)\cos\delta\sin\delta & 0\\ (I_1-I_2)\cos\delta\sin\delta & I_1\sin^2\delta+I_2\cos^2\delta & 0\\ 0 & 0 & I_3\end{pmatrix},\tag{2.5}$$

where $I_1, I_2$ and $I_3$ are the principal moments of inertia of the stone.

We express the vectors $\boldsymbol{r}$, $\dot{\boldsymbol{r}}$ and $\boldsymbol{\omega}$ by $\boldsymbol{M}$ and $\boldsymbol{\gamma}$ using relations (2.2), (2.4) and (2.5). Then the system (2.1) can be represented in the standard form of a six-dimensional system with respect to the phase variables $\boldsymbol{M}$ and $\boldsymbol{\gamma}$:

$$(\dot{\boldsymbol{M}}, \dot{\boldsymbol{\gamma}}) = G(\boldsymbol{M}, \boldsymbol{\gamma}, \mu), \tag{2.6}$$

which also depends on the parameters $\mu$ characterizing the geometrical and physical properties of the stone. Note that on the common level set of the integrals (2.3) the system (2.1) defines the flow on a four-dimension manifold: $\mathcal{M}^3 = \{(\boldsymbol{M}, \boldsymbol{\gamma}) : (\boldsymbol{\gamma}, \boldsymbol{\gamma}) = 1, \mathcal{H}(\boldsymbol{M}, \boldsymbol{\gamma}) = \text{const}\}$, homeomorphic to $\mathbb{S}^3 \times \mathbb{S}^3$.

**Remark 2.** Note that the explicit form of the system (2.6) is rather unwieldy, therefore, we do not present it here. The detailed description how to obtain this system can be found in [26, Section 2]. However, exactly this formula (in the variables $\boldsymbol{M}$ and $\boldsymbol{\gamma}$) is integrated in the software package "Chaos". We emphasize that the Andoyer–Deprit variables, see Section 2.1, are only used for graphical representations of the Poincaré map.

### *2.1. The Andoyer–Deprit variables*

In numerical investigations of the dynamics of the Celtic stone we use the so-called *Andoyer–Deprit* variables $(L, H, G, g, l)$ defined by the formulae [25]

$$\begin{aligned}
&M_1 = \sqrt{G^2 - L^2}\sin l, \quad M_2 = \sqrt{G^2 - L^2}\cos l, \quad M_3 = L,\\
&\gamma_1 = \left(\frac{H}{G}\sqrt{1 - \frac{L^2}{G^2}} + \frac{L}{G}\sqrt{1 - \frac{H^2}{G^2}}\cos g\right)\sin l + \sqrt{1 - \frac{H^2}{G^2}}\sin g \cos l,\\
&\gamma_2 = \left(\frac{H}{G}\sqrt{1 - \frac{L^2}{G^2}} + \frac{L}{G}\sqrt{1 - \frac{H^2}{G^2}}\cos g\right)\cos l - \sqrt{1 - \frac{H^2}{G^2}}\sin g \sin l,\\
&\gamma_3 = \frac{HL}{G^2} - \sqrt{1 - \frac{L^2}{G^2}}\sqrt{1 - \frac{H^2}{G^2}}\cos g.
\end{aligned} \tag{2.7}$$

By definition (see, e.g., [25]),

$$H = (\boldsymbol{M}, \boldsymbol{\gamma}) = M_1\gamma_1 + M_2\gamma_2 + M_3\gamma_3. \tag{2.8}$$

On the common level set of two integrals (2.3), the system (2.6) represents a four-dimensional flow $\mathcal{G}_E$. Note that the new coordinates $L, H, G, g$ and $l$ are chosen in such a way that the condition $(\boldsymbol{\gamma}, \boldsymbol{\gamma}) = 1$ holds automatically. Thus, the formulae (2.7) specify a one-to-one correspondence between the coordinates $\{(\boldsymbol{M}, \boldsymbol{\gamma}) : \boldsymbol{\gamma}^2 = 1\}$ and $(L, H, G, g, l)$ everywhere except for the planes $L/G = \pm 1$ and $H/G = \pm 1$ (in which the coordinate $l$ and, respectively, $g$ are not defined).

Further, we will investigate the systems on the four-dimensional energy levels $\mathcal{H}(L, G, H, l, g) = E$. In this case the planes $g = g_0 = \text{const}$ (for appropriate $g_0$) can be considered as cross-sections for orbits of the corresponding four-dimensional flow $\mathcal{G}_E$. Thus, we can also study the dynamics of a three-dimensional Poincaré map [7, 8]:

$$\bar{x} = \mathcal{F}_{g_0}(x), \quad x = \left(l, \frac{L}{G}, \frac{H}{G}\right), \tag{2.9}$$

which is defined in the domain $0 \leqslant l < 2\pi, -1 < \frac{L}{G} < 1, -1 < \frac{H}{G} < 1$.

### *2.2. Symmetries in the Celtic Stone Model*

The system (2.6) possesses a number of interesting and useful symmetries described by the following lemma.

**Lemma 1 ([8]).** *In the case under consideration, the system (2.6) is symmetric with respect to the coordinate changes:*

$$(a) \qquad \mathcal{S}_1 : \ \omega \to -(-\omega_1, -\omega_2, \omega_3) \ , \ \ \gamma \to (-\gamma_1, -\gamma_2, \gamma_3) \tag{2.10}$$

*and is reversible with respect to the following involutions:*

$$\begin{aligned} &(b) \qquad \mathcal{I}_1 : \ \omega \to -\omega, \ \ , \ \ \gamma \to \gamma, \ \ , \ \ t \to -t \\ &(c) \qquad \mathcal{I}_2 : \ \omega \to (\omega_1, \omega_2, -\omega_3) \ , \ \ \gamma \to (-\gamma_1, -\gamma_2, \gamma_3), \ \ t \to -t. \end{aligned} \tag{2.11}$$

Note that these symmetries and involutions are also preserved for the Andoyer–Deprit coordinates. However, they cannot always be linear in this case. But for the Poincaré map (2.9) with the cross-section $g = 0$, which we denote as $\mathcal{F}_0$, the symmetries (2.11) remain linear.

**Lemma 2 ([8]).** *The map $\mathcal{F}_0$ is invariant under the following transformations:*

$$\begin{aligned} &(a) \qquad \tilde{\mathcal{S}}_1 : \ \ l \to l + \pi, \ \ \frac{L}{G} \to \frac{L}{G}, \ \ \frac{H}{G} \to \frac{H}{G}, \\ &(b) \ \tilde{\mathcal{I}}_1 : \ l \to l + \pi, \ \ \frac{L}{G} \to -\frac{L}{G}, \ \ \frac{H}{G} \to -\frac{H}{G}, \ \ \mathcal{F}_0 \to \mathcal{F}_0^{-1}, \\ &(c) \ \tilde{\mathcal{I}}_2 = \tilde{\mathcal{I}}_1 \tilde{\mathcal{S}}_1 : \ l \to l, \ \ \frac{L}{G} \to -\frac{L}{G}, \ \ \frac{H}{G} \to -\frac{H}{G}, \ \ \mathcal{F}_0 \to \mathcal{F}_0^{-1}. \end{aligned} \tag{2.12}$$

**Corollary 1.** *Let $\mathcal{F}_0$ have an orbit $L^*$. Then $\tilde{S}_1(L^*)$, $\tilde{\mathcal{I}}_1(L^*)$ and $\tilde{\mathcal{I}}_2(L^*)$ are also orbits of $\mathcal{F}_0$. Moreover, the orbits $L^*$ and $\tilde{S}_1(L^*)$, as well as $\tilde{\mathcal{I}}_1(L^*)$ and $\tilde{\mathcal{I}}_2(L^*)$, are symmetric with respect to each other. The orbits $L^*$ and $\tilde{S}_1(L^*)$ are both in involution with the orbits $\tilde{\mathcal{I}}_1(L^*)$ and $\tilde{\mathcal{I}}_2(L^*)$.*

## 3. BIFURCATIONS AND CHAOTIC DYNAMICS OF THE BM-STONE

In this section we consider the model of a Celtic stone having the following geometrical and physical parameters: [3)]

$$I_1 = 5, I_2 = 6, I_3 = 7, m = 1, \mathrm{g} \ = 100, a_1 = 9, a_2 = 4, h = 1 \ \text{ and } \ \delta = 0,2 \tag{3.1}$$

Thus, we study the same model as in [7, 8], see also [26, Section 4] and [32]. We consider the one-parameter families of four-dimensional flows (2.6) or three-dimensional maps (2.9) with the governing parameter $E$.

Denote the one-parameter families of the flows (2.6) and the maps (2.9) as $\mathcal{G}_E$ and $\mathcal{F}_{0E}$, respectively. As was shown in [7, 8], the dynamics of system $\mathcal{G}_E$ is quite simple at large values of $E$. The system has two equilibria $O_1$ and $O_2$ corresponding to permanent rotations about the vertical axis $\gamma = (0, 0, 1)$ with angular frequencies $\omega_1 = (0, 0, \omega_0)$ and $\omega_2 = (0, 0, -\omega_0)$. At $E > E_2 > 1300$ the equilibrium $O_2$ is asymptotically stable and, hence, $O_1$ is completely unstable[4)].

**Remark 3.** For the vertical rotation we have $E = \frac{1}{2} I_3 \omega_0^2 + mgh$, which implies that $\omega_0 = \sqrt{2(E - mgh)/I_3}$.

As $E$ decreases, certain bifurcations occur. At first, they are related to changes of the stability regimes: the loss of stability of the equilibrium $O_2$ and the appearance of new attractors (repellers). Next, the bifurcations lead to the emergence of complex dynamics and chaos (associated with strange attractors, mixed dynamics or almost conservative non-integrable dynamics). This is followed eventually by dynamical behavior close to integrable one (when the values of energy are close to potential $E = 100$). Below we describe the corresponding bifurcations in detail.

---

[3)] The linear sizes are represented here in centimeters, time in sec/$\sqrt{10}$ , weight in kilograms (in particular, the gravity acceleration g is equal to 100 as the standard $10m/sec^2$ is transformed into $100m/\{(\sqrt{10}\mathrm{sec})^2\}$).

[4)] However, stones for which both equilibria are always unstable (saddle-foci) are also known [2, 8]. An example of such Celtic stone is presented in [8]. In this case $I_1 = 4, I_2 = 5, I_3 = 6$, whereas for the stone under consideration we have $I_1 = 5, I_2 = 6, I_3 = 7$. Note that for such stones the Andronov–Hopf bifurcation goes from infinity, thus, a stable vertical rotation occurs here with a small precession (the larger the value of energy, the smaller the precession).

### 3.1. Bifurcations in Regular Dynamics

At $E = E_2 = 1300$ the equilibrium $O_2$ loses stability under the soft (supercritical) Andronov–Hopf bifurcation and a stable limit cycle is born in its neighborhood, which we will call the *K-cycle*.[5] At the same time, a completely unstable limit cycle is born due to reversibility in a neighborhood of $O_1$; the points $O_1$ and $O_2$ become simultaneously saddle-foci of type $(2, 2)$.[6]

Note that the $K$-cycle loses its stability at $E = E_3 \sim 935$ under a saddle-node bifurcation: the $K$-cycle collides at $E = E_3$ with a saddle limit cycle of the same period, and both disappear. However, another stable regime is immediately observed after that — an asymptotically stable limit cycle, [8], which we will call the $BM$-cycle.

**Remark 4.** The stable $K$-cycle is unique (and hence $\mathcal{S}_1$-symmetric). Concerning the stable $BM$-cycles, two of them are born at the same time, $C_1$ and $C_1' = \mathcal{S}_1(C_1)$, symmetric with respect to each other; therefore, there also exist two completely unstable $BM$-cycles — $\tilde{C}_1 = \mathcal{I}_2(C_1)$ and $\tilde{C}_1' = \mathcal{I}_1(C_1)$, see Fig. 1.

We tracked the evolution of the stable $BM$-cycle(s) as $E$ increased. It loses stability at $E = E_1 \sim 1510$, under a soft Neimark–Sacker bifurcation: at $E < E_1$ the cycle is stable, at $E > E_1$ it becomes a cycle of saddle-focus type (with one stable and two complex-conjugate unstable multipliers) and an attracting two-dimensional invariant torus is born. Note that this torus preserves stability for a narrow range of $E$: for $E > E_{tor} \sim 1550$ it becomes a torus of saddle type as well. We did not consider the existence of other stable regimes for higher ($E > 1500$) values of energy.

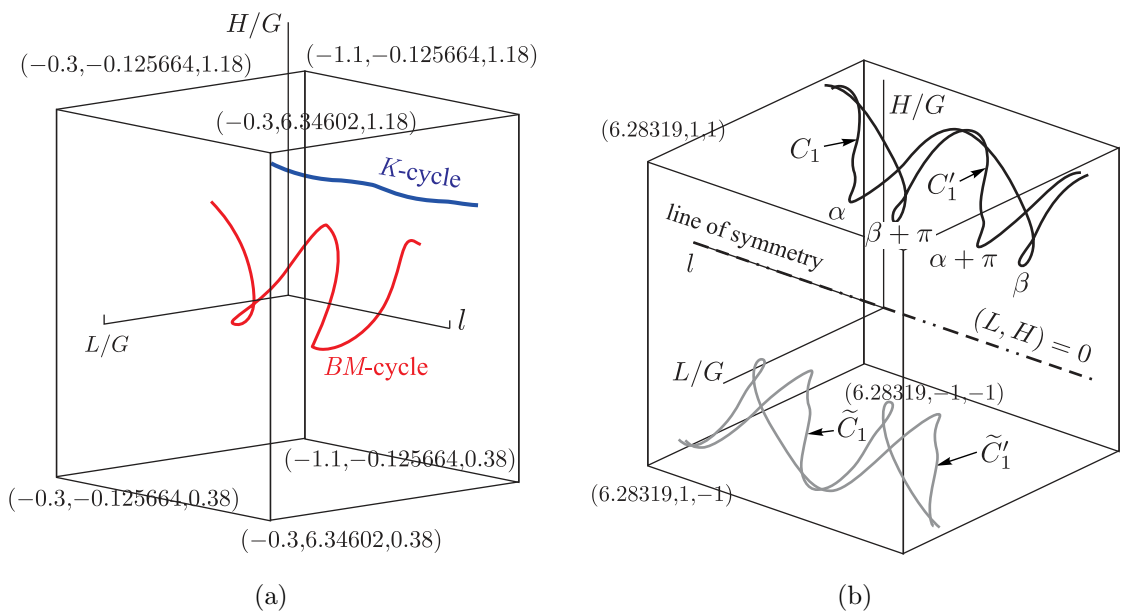


**Fig. 1.** Projections of the limit cycles onto the three-dimensional section $g = 0$: (a) a stable $K$-cycle and one of the $BM$-cycles at $E = 1100$; (b) four $BM$-cycles: two stable and two completely unstable cycles at $E = 600$.

**Remark 5.** For $E_1 > E > E_3$ the system is *multistable*, as three attractors exist in it. At $E_1 > E > E_2$ they are the equilibrium $O_2$ and two $BM$-cycles $C_1$ and $C_1'$ and at $E_2 > E > E_3$ the stable limit cycles, $K$-cycle and two $BM$-cycles.[7]

---

[5] Note that this bifurcation was first studied by A. V. Karapetyan in [27].

[6] The point $O_2$ has the characteristic roots $\nu_{1,2} = -\lambda_1 \pm i\mu_1, \nu_{3,4} = \lambda_2 \pm i\mu_2$, where $\mu_i > 0, i = 1, 2$, $\lambda_1 > 0$ and and $\lambda_2 < 0$ if $E > E_2$, $\lambda_2 = 0$ at $E = E_2$ and $\lambda_2 > 0$ if $E < E_2$. Accordingly, the equilibrium $O_1$ has the characteristic roots of $\nu_{1,2} = \lambda_1 \pm i\mu_1, \nu_{3,4} = -\lambda_2 \pm i\mu_2$.

[7] In the experiment one can expect the following. With the initial vertical clockwise rotation with frequencies $(0, 0, -\omega_0)$ this rotation will be preserved at $E_1 > E > E_2$ or will keep its direction and have a slight precession

### 3.2. The Onset of Chaos

The limit BM-cycles $C_1$ and $C_1'$ lose their stability simultaneously at $E = E_4 \sim 561$ under a period-doubling bifurcation. This loss of stability is *sharp* (or catastrophic, or dangerous), since the stable $BM$-cycle collides at $E = E_4$ with a double-period saddle cycle and becomes a cycle of saddle type at $E < E_4$. Moreover, chaotic dynamics — something like a "strange attractor" — is observed immediately after that. Note that the value $E = E_4$ is close to the moment of creation of a homoclinic loop to the saddle-focus $O_2$. This gives rise to complex dynamics [28], where stable $BM$-cycles exist, but it is not attractive in this case. Due to reversibility, for $E < E_4$ there also exists a "strange repeller". At the instant close to the moment of bifurcation the attractor and the repeller are definitely separated, as is evident from the numerical calculations in Fig. 2a.

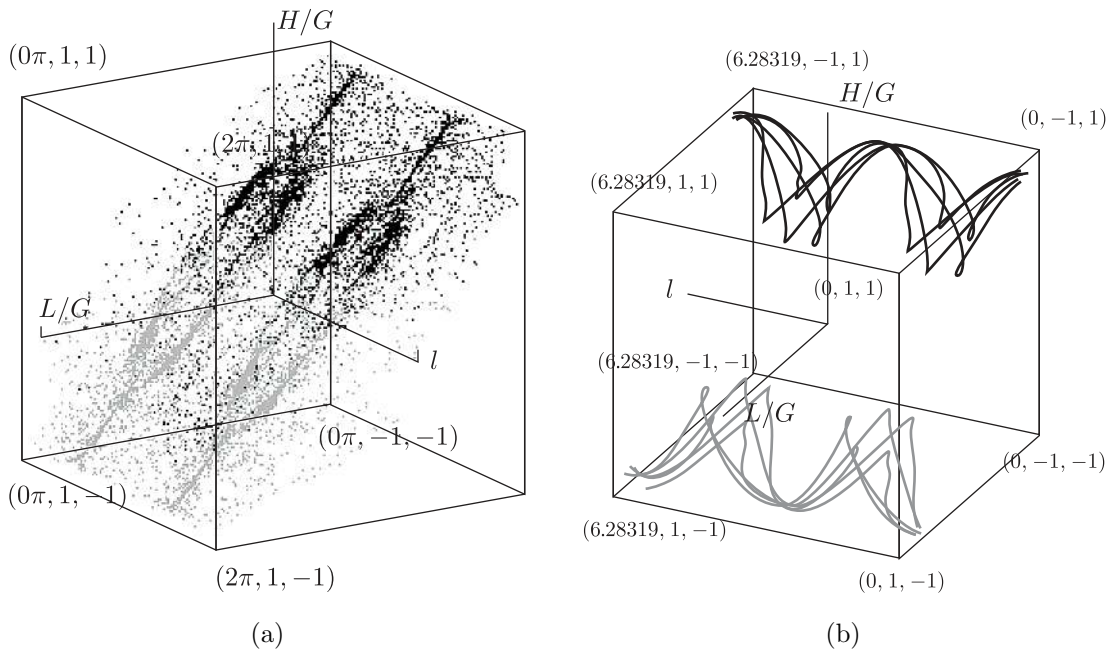


**Fig. 2.** (a) $E = 555$, the attractor (black) and the repeller (grey) are definitely separated; (b) the stability window: the stable limit cycle of period 5 (black) and the completely unstable cycle (grey) symmetric with respect to it at $E = 510$.

Note that the observed chaos is certainly not hyperbolic due to the presence or appearance of stable periodic orbits under small perturbations of the homoclinic tangencies or non-transversal heteroclinic cycles (contours) etc. In such cases, a change in the parameters usually leads to the appearance of the so-called "stability windows", i.e., open sets in the parameter space in which the attractor is a periodic orbit. Such a stability window was observed in our model: at $528 > E > 485$ the attractor is a stable limit cycle of period 5, see Fig. 2b. Due to a further decrease in the values of $E$ this cycle undergoes a series of period-doubling bifurcations (we observed several of them) and then a SA appears again.

The chaos is spiral over a sufficiently wide range of values of the parameter ($470 > E > 350$) because the saddle-focus belongs to the attractor (which is obtained numerically), see Fig. 3a. This means automatically that the saddle-focus $O_1$ belongs to the repeller at the same moment.

With further decrease in $E$ the observable attractor and repeller may significantly "mix" so that the limit regimes for backward and forward iterations will be hard to distinguish. In other words, the phenomenon of *mixed dynamics* may be observed here (see also the Introduction) when

at $E_2 > E > E_3$ (the motion along the $K$-cycle). With the initial counter-clockwise rotation corresponding to the frequencies $(0, 0, \omega_0)$, this rotation due to the system's reversibility will change its direction at $E_1 > E > E_3$ but a precession with a higher magnitude than that in the previous case may occur (the motion along one of the $BM$-cycles).

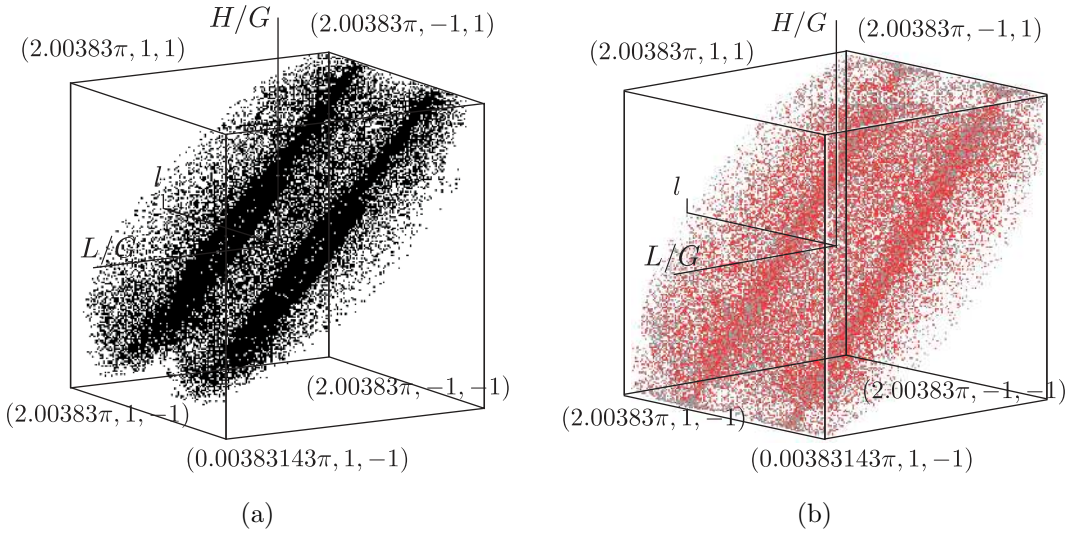


**Fig. 3.** (a) $E = 470$, a spiral attractor; (b) mixed dynamics at $E = 320$.

hyperbolic periodic orbits of various types (stable, completely unstable and saddle) and elliptic orbits coexist and, generically, they are not separable from each other.

Specifically, the mixed dynamics takes place when both saddle-foci $O_1$ and $O_2$ (with positive and negative divergence, respectively) belong to the closure of the limit set to which the orbits tend as $t \to +\infty$ (hence, due to the reversibility, they also belong to the closure of the limit set to which the orbits tend as $t \to -\infty$). In Fig. 3b, a picture of the attractor and the repeller of map $\mathcal{F}_E$ is shown for $E = 320$, which consists of about 20000 points, of which 10000 (red) have been obtained for forward iterations and the other 10000 (grey) for backward iterations of the map (the total number of forward and backward iterations counted by us was 50000, but the first 40000 ones were ignored). In the average, the limit set appears to be "pink". Note that some kind of asymmetry may occur here during forward and backward iterations if asymptotically stable and asymptotically unstable periodic orbits symmetric with respect to each other are present in the dynamics of the map $\mathcal{F}_{0E}$. However, such orbits have usually very large periods, and therefore the asymmetry can be weak [5].

With further decrease in $E$ the development of conservative chaos is observed. Initially it can be associated with the mixed chaotic dynamics in which the symmetric orbits start to play a key role, see Fig. 4a. Due to them the dynamics becomes more and more similar to integrable conservative dynamics, see Fig. 4b, as $E$ tends to the limit value $E = 100$, which corresponds to the stop of the stone.

### *3.3. A Sketch of Bifurcations and Chaotic Dynamics in the Model of BM-stone*

In this section we represent a "bifurcation tree" from Fig. 5, in which we try to express the main results presented in Sections 3.1 and 3.2. This tree reflects only some important qualitative dynamical properties of the BM-stone model and their changes as the parameter $E$ varies.

The main bifurcations in regular dynamics (discussed in Section 3.1) are also schematically shown. When $E < E_4$, the regular dynamics gives way to chaotic dynamics. In fact, Fig. 5 is a graph with the axes $E$ and $L/G$. The line $L/G = -1$ corresponds to the equilibrium $O_2$, by symmetry, $L/G = +1$ corresponds to $O_1$. The line $L = 0$ corresponds to the line of fixed points of the involution $\tilde{\mathcal{I}}_2$, see formula (2). Therefore, the presented symmetric elements of dynamics for $L > 0$ and $L < 0$ are in involution. Thus, for $L < 0$ and $L > 0$ we have attractors and repellers, respectively.

Concerning the stable regular dynamics, when decreasing $E$ we have the following sequence: the stable equilibrium $O_2$ (for $E < E_2$), a stable 2-torus (for $E_{tor} > E > E_1$), the BM-cycle ($E_1 < E < E_4$) and the K-cycle ($E_2 < E < E_3$). These objects can evidently coexist.

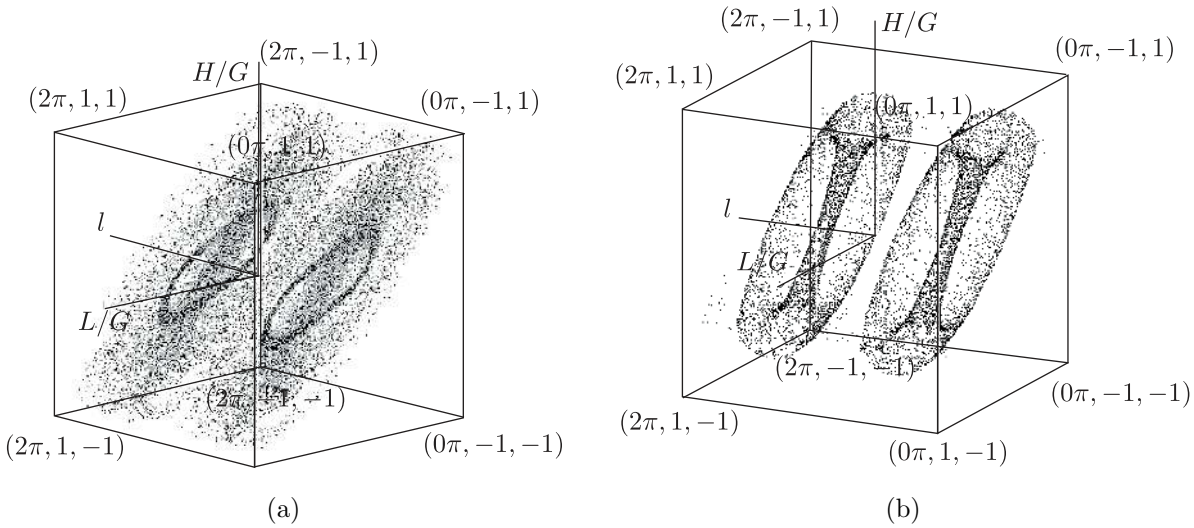


**Fig. 4.** Mixed dynamics at $E = 220$ (a) two-dimensional tori for the Poincaré map at $E = 170$ (b).

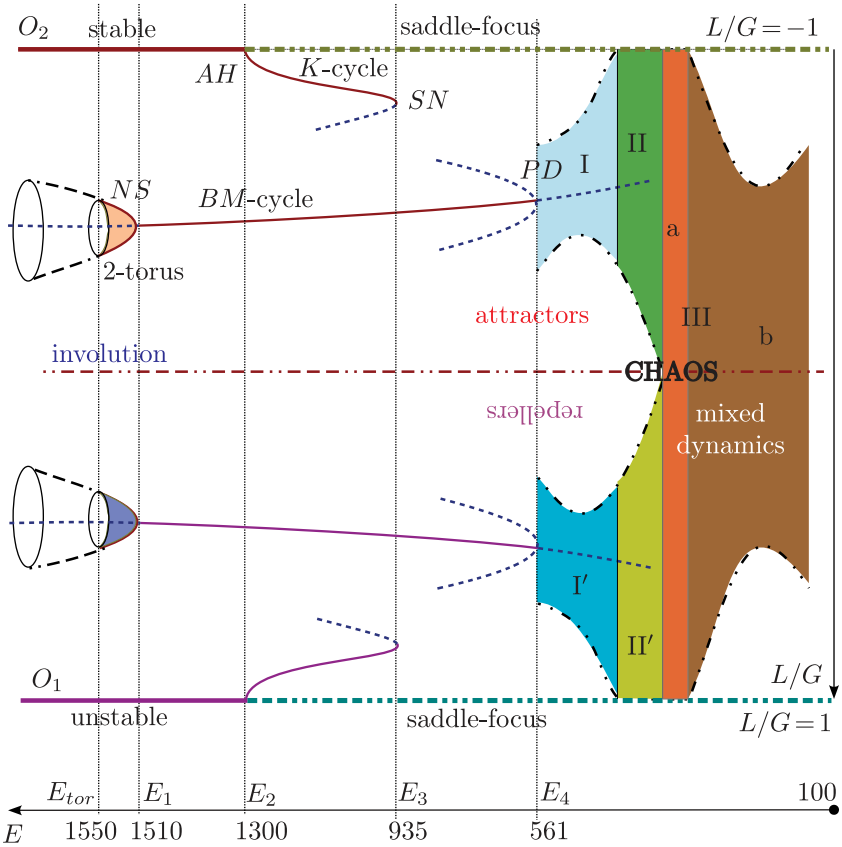


**Fig. 5.** A bifurcation tree for the BM-stone model. We use the following notation here: AH is the Andronov–Hopf bifurcation with an equilibrium state of the flow $\mathcal{G}_E$; NS is the Neimark–Sacker bifurcation, SN is a saddle-node bifurcation, and PD is a period-doubling bifurcation (in this case it is sharp (subcritical)) with a fixed point of the map $\mathcal{F}_{0E}$.

When $E < E_4 \simeq 561$, the chaotic dynamics occurs. We show chaotic zones in Fig. 4 (open domains in the plane $(E, L/G)$ such that, for every fixed $E$, the values of $(L/G)$ range from the minimal to the maximal one on the attractor (repeller)). Strange attractors (repellers) corresponding to zone I (I') (such as in Fig. 2) are not specified by us. Zone II (II') corresponds

to a spiral strange attractor (repeller), such as in Fig. 3. In this case the saddle foci $O_1$ and $O_2$ belong to the attractor and the repeller, respectively. Accordingly, the line $L/G = -1$ adjoins zone II ($L/G = +1$ adjoins II'). The region $\mathrm{III}_a \cup \mathrm{III}_b$ corresponds to the existence of the mixed dynamics. For the region $\mathrm{III}_a$, the type of mixed dynamics is such that both saddle-foci $O_1$ and $O_2$ belong to the chaotic set. Whereas the region $\mathrm{III}_b$ corresponds to another type of mixed dynamics when both saddle-foci $O_1$ and $O_2$ keep of out the chaotic set. Note that as the value $E = 100$ (the potential energy) is approached, the elements of conservative dynamics become more clearly visible.

## 4. ON DISCRETE LORENZ ATTRACTORS IN CELTIC STONE DYNAMICS

In this section we consider the nonholonomic model of a Celtic stone whose physical parameters are as follows:

$$I_1 = 2, \quad I_2 = 6, \quad I_3 = 7, \quad m = 1, \quad \mathrm{g} = 100, \quad a_1 = 9, \quad a_2 = 4, \quad h = 1. \tag{4.1}$$

We also take $\delta = 0.485$. Note that this model only differs from the model of BM-stone by the values given to $I_1$ and $\delta$.

Note that the Celtic stone model with the parameters (4.1) was considered in [33] in which a SA was found, at $E = 770, \delta = 0.405$, to be quite similar to the attractor from Fig. 10f. Since analogous attractors are known to exist in three-dimensional Hénon maps [34, 41] near the boundaries of destruction of discrete Lorenz attractors, the question naturally arises whether a discrete Lorenz attractor exists for close values of the parameters $E$ and $\delta$. The answer is positive and we give here a short review of results obtained.

We study, using both qualitative and numerical methods, bifurcations in the family $\mathcal{F}_{0E}$ of the Poincaré map $\mathcal{F}_{0E}$ (2.9) for appropriate values of $E$ (with fixed $\delta = 0.485$). We will act by employing the following strategy (its justification is given in the Appendix, Section 4).

1) We verify the geometrical similarity of our attractor $A_{E^*}$ found in the Celtic stone model to the Lorenz attractor. Here the strange attractor which was found for $E = E^* = 752$ is examined.

In particular, this similarity manifests itself in the fact that our three-dimensional map $\mathcal{F}_{0E^*}$ possesses the following features: (i) it has a fixed saddle point $O^*$ belonging to the attractor $A_{E^*}$ with the multipliers of $\lambda_1, \lambda_2, \gamma$ such that $|\lambda_2| < |\lambda_1| < 1 < |\gamma|$, $\lambda_1 > 0, \lambda_2 < 0, \gamma < -1$ and $|\lambda_1\gamma| > 1$; (ii) the manifolds $W^u(O)$ and $W^s(O)$ have a nonempty intersection; (iii) the phase portraits look "similar", see Fig. 6.

We mention that negative values of the multipliers $\lambda_2$ and $\gamma$ provide the Lorenz symmetry ($x \to x, y \to -y, z \to -z$) of the homoclinic structure. Moreover, for the values of the parameter $E$ close to $E^*$, the manifold $W^u$ will intersect $W^s$ strictly from one side of the strong stable invariant manifold $W^{ss}(O)$, which is tangent to the eigendirection corresponding to the multiplier $\lambda_2$ of $O^*$, which provides the "homoclinic configuration of a figure-eight-butterfly" similar to the Lorenz attractor.

2) Verify numerically the strangeness and pseudo-hyperbolicity of the attractor $A_{E^*}$ (we refer to Section 4 for the definition of pseudo-hyperbolicity and related terms).

At this stage we investigate the spectrum $\Lambda_1, \Lambda_2, \Lambda_3$ of the Lyapunov exponents of the map $\mathcal{F}_{0E^*}$ on the attractor $A^*$ and show that this spectrum, where $\Lambda_1 > \Lambda_2 > \Lambda_3$, satisfies the following conditions: (1) $\Lambda_1 > 0$; (2) $\Lambda_1 + \Lambda_2 + \Lambda_3 < 0$; (3) $\Lambda_1 + \Lambda_2 > 0$. The conditions (1) and (2) imply that the attractor $A^*$ is strange and the condition (3) implies that it is pseudo-hyperbolic (the map expands areas in two directions transversal to the strong contraction related to the exponent $\Lambda_3 < 0$).

3) Plot numerically the graph of the maximal exponent $\Lambda_1 = \Lambda(E)$ for some range of the parameter $E$ containing this value, $E = E^*$, for which the attractor $A_{E^*}$ exists, see Fig. 7.

At this stage we verify (only numerically) that our attractor is not a quasi-attractor, i.e., it does not contain stable periodic orbits of large periods, which do not appear under perturbations either. As is seen from Fig. 7, the graph resides in the domain $\Lambda_1 > 0$ and looks like a continuous function, whereas, if $A_{E^*}$ were a quasi-attractor, the "holes" would be observed on the plot containing the ranges of $\Lambda_1 < 0$ corresponding to "stability windows".

4) Investigate (mostly numerically) the main bifurcations starting at a stable fixed point and leading to the appearance of discrete Lorenz attractors (including $A_{E^*}$). We also trace the main stages of destruction of SA.

In principle, this item may seem unnecessary but we suppose it to be the most interesting as here one can follow a certain "genetic" connection between the phenomena observed in flows with the Lorenz attractors (Lorenz model, Shimizu–Morioka model etc.) and those observed in the model of a Celtic stone. Moreover, as the calculations show, our Poincaré map $\mathcal{F}_{0E}$ behaves like a "small perturbation of the time shift of a flow from the geometric Lorenz model" for corresponding values of $E$. Formally, this circumstance can be caused by the interesting fact that the middle Lyapunov exponent $\Lambda_2$ is very close to zero (for the flow case it is simply equal to zero): during calculations it demonstrates small oscillations in the range between 0.00007 and 0.00015, see [22] for a discussion of this topic. But what is really interesting is that the bifurcations leading to the appearance of SA are here almost identical to those which accompany the birth of SA in the Lorenz model [31], see. Fig. 8b–8f.

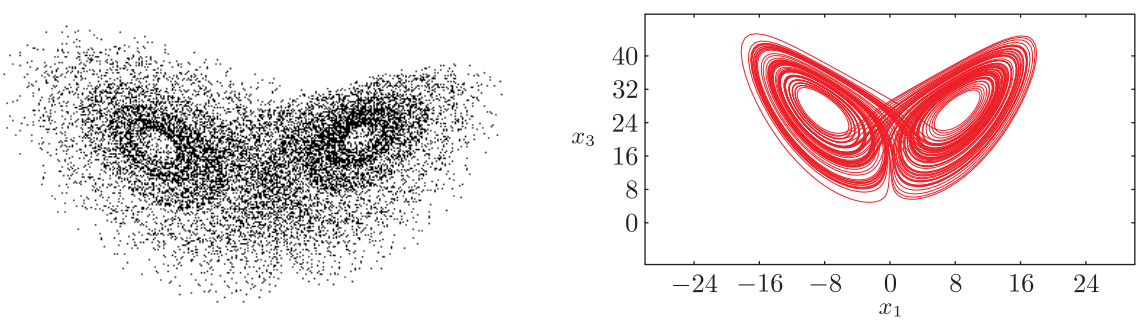


(a) (b)

**Fig. 6.** (a) a Lorenz-like attractor for $E = E^* = 752$ in the Celtic stone model with the set of parameters (4.1) (about 10000 iterations of some initial point are shown); b) the projection of the Lorenz attractor from the Lorenz model onto the $(x, z)$ plane.

Below we show the results of numerical investigations performed according to items 1)–4) of the strategy.

1) Figure 6 shows (a) iterations of a single point of the attractor $A_{E^*}$ of the map $T_E$ for $E = E^* = 752$ (for an appropriate angle of projection) and (b) the projection of orbits of the classical Lorenz attractor from the Lorenz model for $r = 28$, $\sigma = 10$, and $b = 8/3$ onto the $(x, z)$ plane displayed for comparison.

The fixed saddle point $O^*$ with the coordinates of $l = 3.650$; $L/G = 0.669$; $H/G = -0.384$ on the attractor $A_{E^*}$ has the multipliers $\lambda_1 = 0.996$; $\lambda_2 = -0.664$; $\gamma = -1.312$. If one draws its unstable manifolds ("separatrices"), then, as expected, they will have "loops" (due to the existence of the homoclinic intersection), see Fig. 9a, in contrast with the unstable separatrices of the Lorenz attractor in flows which appear to be sufficiently monotonous spirals.

2) For the attractor $A_{E^*}$ at $E = E^* = 752$ the spectrum of the Lyapunov exponents was obtained as follows: $\Lambda_1 = 0.0248$; $\Lambda_3 = -0.2445$, $0.00007 < \Lambda_2 < 0.00015$.

Evidently, the conditions $\Lambda_1 > 0$, $\Lambda_1 + \Lambda_2 + \Lambda_3 < 0$ and $\Lambda_1 + \Lambda_2 > 0$ hold here.

3) On the graph of Fig. 7 the dependence of the maximal Lyapunov exponent $\Lambda_1 = \Lambda_1(E)$ on $E$ is shown for the range $[752; 752.01]$ of the parameter $E$.

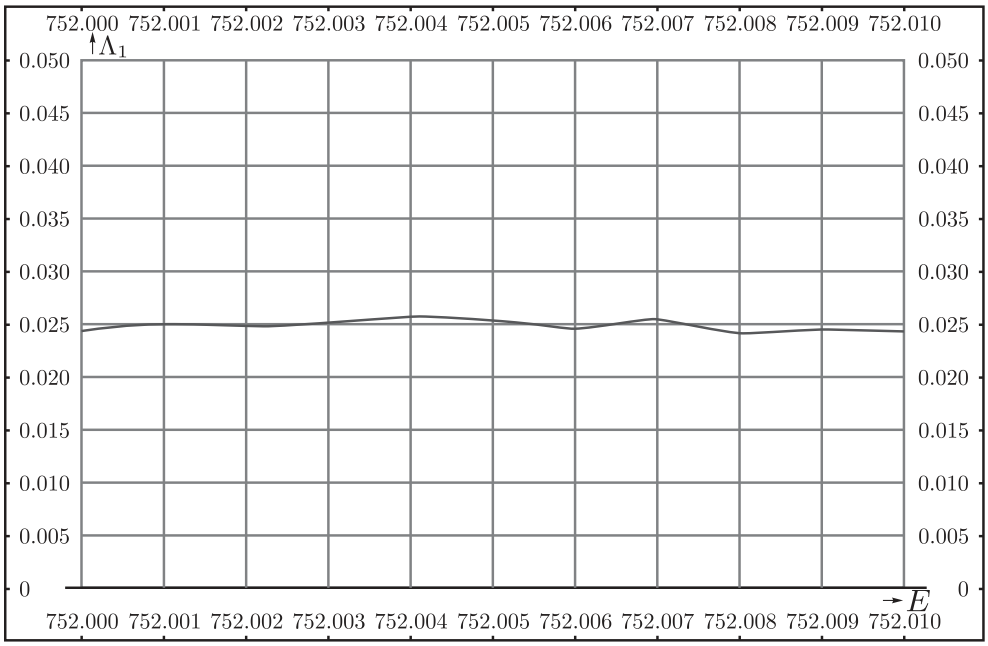


**Fig. 7.** The plot of $\Lambda_1(E)$ in the range of $[752; 752.01]$.

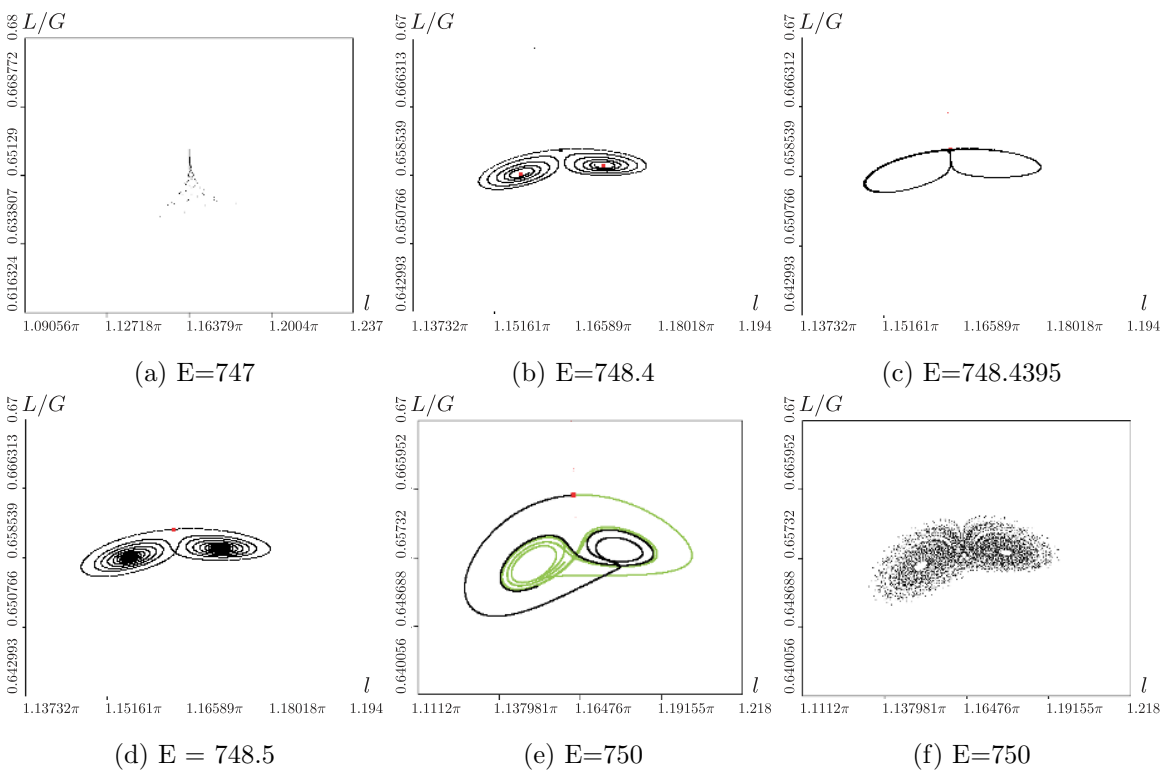


**Fig. 8.** The main stages of evolution of the Lorenz-like attractor in the map $T_E$. Figures a) and e) show iterations of some starting point, and Figs. b)–g) show unstable manifolds (separatrices) of the fixed point $O$.

4) Figure 8 illustrates the main stages of evolution of a discrete Lorenz attractor in the map $\mathcal{F}_{0E}$ for the parameter $E$ growing from $E = 747$ to $E = E^* = 750$.

Initially the attractor is a stable fixed point $O$, Fig. 8a. Then, at $E = E_1 = 747.61$, it undergoes a period-doubling bifurcation and the stable cycle $P = (p_1, p_2)$ of period two becomes an attractor,

Fig. 8b. At $E = E_2 = 748.4395$ a "homoclinic figure-eight-butterfly" of the unstable manifolds (separatrices) of the saddle $O$ is created, Fig. 8c, which then gives rise to a saddle-type closed invariant curve $L = (L_1, L_2)$ of period two (where $\mathcal{F}_{0E}(L_1) = L_2, \mathcal{F}_{0E}(L_2) = L_1$), the curves $L_1$ and $L_2$ surround the point $p_1$ and $p_2$, respectively. At the same time, the unstable separatrices of $O$ are rebuilt and now, for $E_2 < E < E_3$, the left (right) one is coiled around the right (left) point of the cycle $P$, Fig. 8d. Moreover, together with the closed period-2 invariant curve $L$, an invariant limit set $\Omega$ is born here here, [31], which is not attracting yet. As the numerical calculations show, for $E = E_3 \sim 748.97$ the separatrices "lie" on the stable manifold of the curve $L$ and then leave it. Almost immediately after that, at $E = E_4 \sim 748.98$, the period-2 cycle $P$ sharply loses stability under a subcritical torus-birth bifurcation: the closed invariant curve $L$ merges with the cycle $P$, after that the cycle becomes a saddle and the curve disappears. The value of $E = E_4$ is the bifurcation moment of the creation of SA — the invariant set $\Omega$ becomes attracting. Even for the parameter values close to $E = E_3$ (and $E > E_3$) the separatrices start to unwind, see Fig. 8e and their configuration becomes similar to the Lorenzian one, which also applies to the phase portrait, see Fig. 8f.

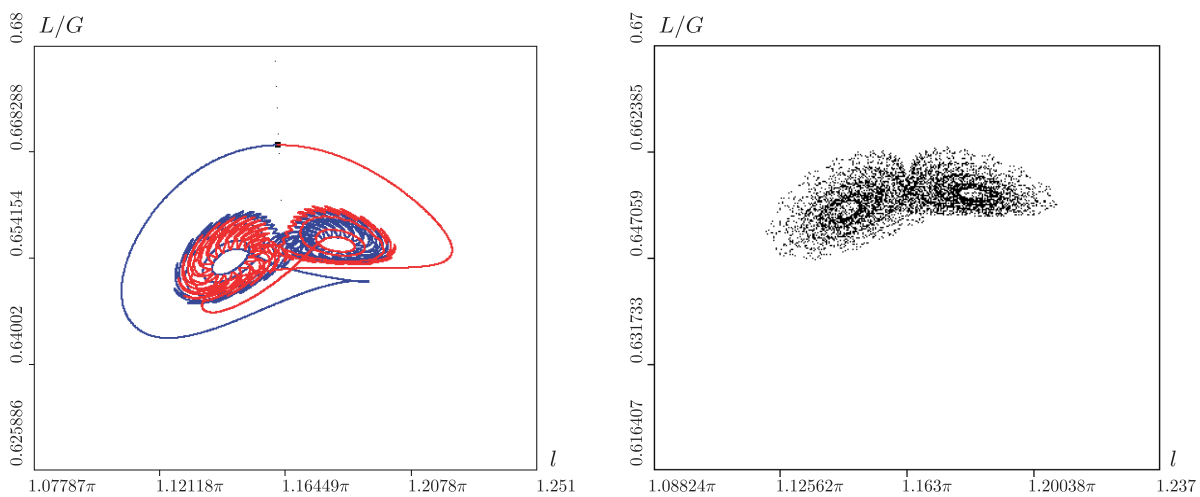


(a) (b)

**Fig. 9**

Figure 9 shows the behavior of (a) manifolds $W^u(O^*)$ and (b) iterations of the points on the attractor $A^*$ of map $\mathcal{F}_{0E^*}$ (here $E = E^* = 752$). This attractor is studied in items 1)–3) above.

Figure 10 shows some stages of destruction of the discrete Lorenz attractor, which is related to the appearance of resonant stable invariant curves , (b), (d) and (e), and the chaotic regimes (torus-chaos), (c) and (f). Note that for $E > 790$ "nothing is left" from the discrete Lorenz attractor and the orbits run away from its neighborhood, tending to a new stable regime — the spiral attractor, observed in [32, 33].

## APPENDIX. TOWARDS THE DEFINITION OF THE DISCRETE LORENZ ATTRACTOR

The Lorenz attractors for flows play a special role in the theory of dynamical chaos. Until recently, these and hyperbolic attractors were the only ones which were classified as "genuine" strange attractors, which, in particular, do not allow the appearance of stable periodic orbits under small perturbations. After publication of the paper [20] by Turaev and Shilnikov the situation changed drastically. They not only provided an example of a wild hyperbolic spiral attractor that must be regarded as a genuine SA but also introduced a new class of *pseudo-hyperbolic attractors*. Thus, a new trend related to the study of such strange attractors appeared in the theory of dynamical chaos.

Below we will give the definition of pseudo-hyperbolicity for diffeomorphisms, which is, in fact, a reformulation of the corresponding definition for flows from [21].

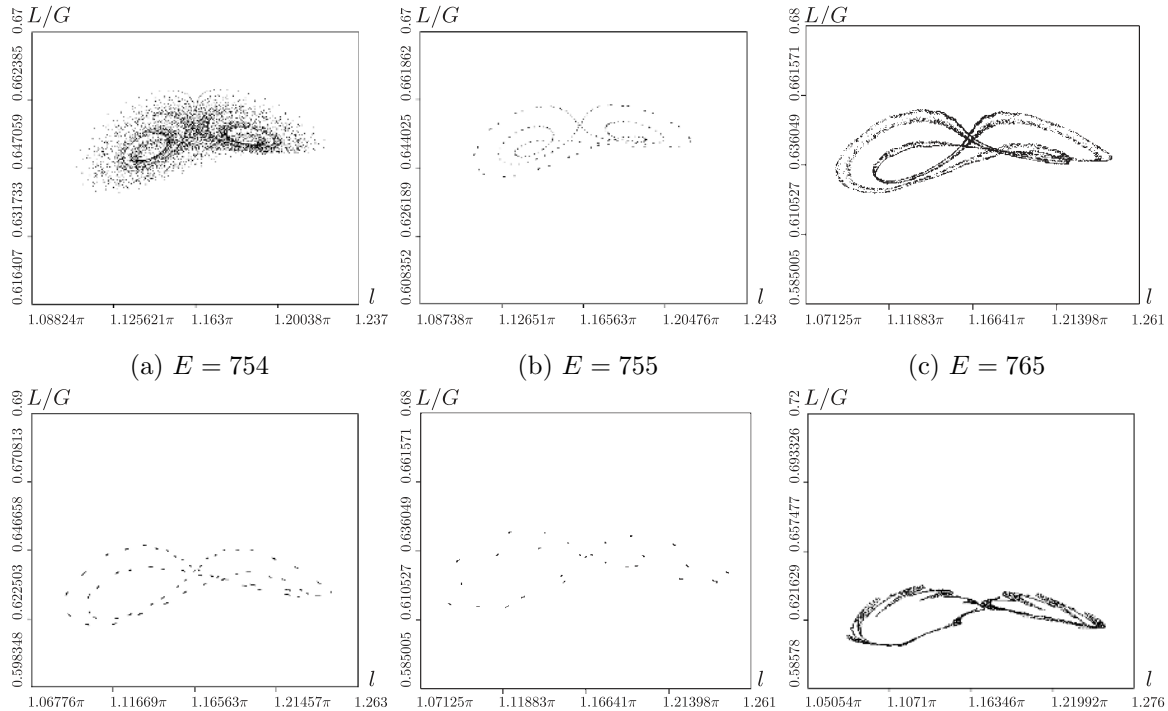


(a) $E = 754$ (b) $E = 755$ (c) $E = 765$

(d) $E = 770$ (e) $E = 775$ (f) $E = 780$

**Fig. 10.** Certain stages of destruction of the discrete Lorenz attractor; a) this is definitely a discrete Lorenz attractor; b) a resonant invariant curve with the period more than 160; c) a strange attractor of torus-chaos type close to the break-down of an invariant curve ($\Lambda_1 = 0.009$); d) an invariant curve with the rotation number $\rho = 29/62$; e) an attractive resonant invariant curve with $\rho = 15/28$; f) a strange attractor of torus-chaos type with $\Lambda_1 = 0.090$ (such strange attractors appear after break-down of an invariant two-dimensional torus (closed invariant curve), by the Afraimovich–Shilnikov scenario [42]);

Let $f$ be a $C^r$-diffeomorphism, $r \geqslant 1$ and let $Df$ be its linearization: $Df(x_0) = \left(\frac{\partial f}{\partial x}_{|x=x_0}\right)$. An open bounded domain $\mathcal{D} \subset \mathbb{R}^n$ is absorbing for $f$ if $f(\overline{\mathcal{D}}) \subset \mathcal{D}$.

**Definition 1.** *The diffeomorphism $f$ is called* pseudo-hyperbolic *on $D$ if the following conditions hold.*

1) *For each point of $D$ there exist two transversal subspaces $N_1$ and $N_2$ continuously depending on the point ($\dim N_1 = k \geqslant 1, \dim N_2 = n - k$) which are invariant with respect to $Df$:*

$$Df(N_1(x)) = N_1(f(x)), \quad Df(N_2(x)) = N_2(f(x)).$$

*and for each orbit $L : \{x_i \mid x_{i+1} = f(x_i),\ i = 0, 1, \ldots; x_0 \in D\}$ the maximal Lyapunov exponent corresponding to the subspace $N_1$ is strictly smaller than the minimal Lyapunov exponent corresponding to the subspace $N_2$, i.e., the following inequality holds:*

$$\lim_{n\to\infty} \sup \frac{1}{n} \ln \left( \sup_{\substack{u \in N_1(x_0) \\ \|u\|=1}} \|D^n f(x_0) u\| \right) < \lim_{n\to\infty} \inf \frac{1}{n} \ln \left( \inf_{\substack{v \in N_2(x_0) \\ \|v\|=1}} \|D^n f(x_0) v\| \right). \tag{A.1}$$

2) *The restriction of $f$ to $N_1$ is contracting, i.e., there exist such constants $\lambda > 0$ and $C_1 > 0$ that*

$$\|D^n f(N_1)\| \leqslant C_1 e^{-\lambda n}. \tag{A.2}$$

3) *The restriction of $f$ to $N_2$ expands volumes exponentially, i.e., there exist such constants $\sigma > 0$ and $C_2 > 0$ that*

$$|\det D^n f(N_2)| \geqslant C_2 e^{\sigma n}. \tag{A.3}$$

The following property immediately follows from this definition:

* All the orbits in $\mathcal{D}$ are unstable: each orbit has a positive maximal Lyapunov exponent

$$\Lambda_{max}(x) = \lim_{n\to\infty} \sup \frac{1}{n} \ \ln \ \|D^n f(x)\| > 0$$

Note that the pseudo-hyperbolicity conditions require the expansion of only $(n-k)$ volumes (by the restriction of the diffeomorfism to $N_2$), which makes these conditions different from those for uniform hyperbolicity, where the expansion of full volumes is required. But for the hyperbolicity the following condition must hold: $\|D^{-n}f(N_2)\| < Ce^{-\sigma n}$, i.e., the uniform expansion should be along all directions in $N_2$. Nevertheless, it is possible to establish the following fact in a standard way [20, 35].

** The pseudo-hyperbolicity conditions are not violated under small $C^r$-perturbations of the system. Moreover, the spaces $N_1$ and $N_2$ change continuously.

These two conditions imply that if the diffeomorphism $f$ has an attractor in $\mathcal{D}$, then this attractor is strange and does not contain stable periodic orbits, which do not appear under small perturbations either. In other words, pseudo-hyperbolic attractors appear to be *genuine SA* (in contrast to the so-called quasi-attractors [36], which can contain stable periodic orbits of large periods).

The discrete Lorenz attractors form a certain subclass of the class of pseudo-hyperbolic attractors. Following Turaev and Shilnikov [20, 21], we make an attempt below to give a definition of such attractors.

First of all, we mention that there exist various definitions of an attractor, see, e.g., [37]. Usually a *strange attractor* is defined to be a compact, asymptotically stable, transitive invariant set. However, an attractor is not always transitive and asymptotically stable. For example, such an attractor may not even be present in the geometric Lorenz model [38], which should be regarded as basic in the theory of Lorenz-like attractors. Thus, we will follow a definition of the attractor introduced in [20, 39], which is based on the notion of $\varepsilon$-orbits (Anosov, Ruelle, Conley and others). Recall the corresponding definitions.

**Definition 2.** *Let $f : M \to M$ be a diffeomorphism of a manifold $M$ and let $\rho(x, y)$ be the distance between the points $x, y \in M$. A sequence of points $x_n \in M$ such that*

$$\rho(x_{n+1}, f(x_n)) < \varepsilon, \quad n \in \mathbb{Z},$$

*is called an $\varepsilon$-*orbit *of $f$.*

**Definition 3.** *We will call a point $y$* achievable *from a point $x$ by $\varepsilon$-orbits ($\varepsilon$-achievable) if for any $\varepsilon > 0$ there exists an $\varepsilon$-orbit of the point $x$ passing through the point $y$.*

**Definition 4.** *A compact invariant set $\Lambda$ is called an* attractor *if it is* (i) `chain-transitive`*, i.e., each point of $\Lambda$ is achievable from any other point of this set by $\varepsilon$-orbits which also belong to $\Lambda$ for each sufficiently small $\varepsilon$, and* (ii) `stable`*, i.e., any $\varepsilon$-orbit starting near the set $\Lambda$ never leaves some small neighborhood of this set.*

Note that the attractors defined in this way (according to Ruelle–Turaev–Shilnikov, [20, 39]) keep their main properties under small random perturbations (noises) as well. Concerning the properties of stability, another important notion is often used in the theory.

**Definition 5.** *A* prolongation *of a point $x \in \mathcal{D}$ is the limit invariant set $\mathcal{P}_x$ defined as*

$$\mathcal{P}_x \ = \bigcap_{\varepsilon>0} \ \overline{\bigcup_{\tilde{x}\in\mathcal{L}_\varepsilon} \tilde{x} \cap \mathcal{D}},$$

*where $\mathcal{L}_\varepsilon$ is the set of points of all $\varepsilon$-orbits of $x$. Also, we define the prolongation of some set as a union of prolongations of all its points.*

We would like to mention that the prolongation of any point/set is always a stable ($\varepsilon$-stable) closed invariant set [20, 40]. Then

- *a chain-transitive attractor is always a prolongation of any of its points.*

This important property of the attractor appears to be a theoretical basis of the main "working strategy" for finding the attractors, which is to find a prolongation of an appropriate point and to try to prove that it is chain-transitive. This is not always easy and various numerical methods can provide significant help.

**Definition 6 ([20, 21]).** *A* pseudo-hyperbolic attractor *is a stable chain-transitive invariant set with a uniform pseudo-hyperbolic structure.*

This definition is quite wide. The class of systems with pseudo-hyperbolic attractors includes systems with hyperbolic attractors and those with Lorenz-like attractors.

Note that the dynamical properties of the geometric Lorenz model [38] under small time-periodic perturbations were investigated in [21]. It was also shown that the properties of pseudo-hyperbolicity and chain-transitiveness of a non-perturbed Lorenz attractor hold for a periodically perturbed attractor as well. Thus, the Poincaré map (the map for a period of perturbation) also possesses here a pseudo-hyperbolic attractor $A$, which appears to be a basic example of a *discrete Lorenz attractor*. Note that the saddle equilibrium of the Lorenz attractor will correspond, after perturbations, to a saddle-type fixed point of the corresponding Poincaré map. Hence, the attractor $A$ is exactly the prolongation of this fixed point, and $A$ is always chain-transitive (when the perturbation is small), see [21].

The same conclusions can also be drawn without assuming that the map under consideration is a Poincaré map of a system periodic in time and close to an autonomous one. For this general case the corresponding definition of a discrete Lorenz attractor was given in [41], however, here we do not reproduce it as it is quite complicated and abstract. But the main idea is the following. First a suspension of a diffeomorphism $f$ is considered which is some flow $F_t$. Therefore, the flow $F_t$ is required to satisfy the main conditions (chain-transitiveness, pseudo-hyperbolicity etc.), which hold for the flow with the periodically perturbed Lorenz attractor from the geometric model. These conditions are then verified for the initial map. But this approach is quite hard to implement in practice although it would be appropriate for theoretical investigations. In the present paper, according to the definitions given above, we have used, instead, the strategy of qualitative and numerical study of Lorenz-like attractors described in items 1)–4) of Section 4.

## ACKNOWLEDGMENTS

The authors are grateful to the referee for his very interesting and helpful remarks and A. Borisov, I. Mamaev, I. Ovsyannikov, and D. Turaev for useful comments. This work was supported by the RFBR grants No.11-01-00001, 13-01-00589 and 13-01-97028-povolzhye, the Federal Target Program "Personnel" No.14.B37.21.0361, and by the Federal Target Program "Scientific and Scientific-Pedagogical Personnel of Innovative Russia" (Contract No. 14.B37.21.0863).

## REFERENCES

1. Astapov, I. S., On Rotation Stability of Celtic Stone, *Vestnik Moskov. Univ. Ser. 1. Mat. Mekh.,* 1980, no. 2, pp. 97–100 (Russian).
2. Karapetyan, A. V., On permanent rotations of heavy rigid body on the absolutely rough horizontal plane, *Prikl. Mat. Mekh.,* 1981, vol. 45, no. 5, pp. 808–814 [*J. Appl. Math. Mech.,* 1981, vol. 45, no. 5, pp. 808–814].
3. Markeev, A. P., The Dynamics of a Rigid Body on an Absolutely Rough Plane, *Prikl. Mat. Mekh.,* 1983, vol. 47, no. 4, pp. 575–582 [*J. Appl. Math. Mech.,* 1983, vol. 47, no. 4, pp. 473–478].
4. Markeev, A. P., *Dynamics of a Body Touching a Rigid Surface*, Moscow–Izhevsk: R&C Dynamics, Institute of Computer Science, 2011 (Russian).
5. Kazakov, A. O., Chaotic Dynamics Phenomena in the Rubber Rock-n-Roller on a Plane Problem, *Rus. J. Nonlin. Dyn.,* 2013, vol. 9, no. 2, pp. 309–325 (Russian).
6. Kazakov, A. O., Strange Attractors and Mixed Dynamics in the Unbalanced Rubber Ball on a Plane Problem, *Regul. Chaotic Dyn.,* 2013, vol. 18, no. 5, pp. 508–520.

7. Borisov, A. V. and Mamaev, I. S., Strange Attractors in the Rattleback Dynamics, in *Nonholonomic Dynamical Systems: Integrability, Chaos, Strange Attractors,* A. V. Borisov, I. S. Mamaev (Eds.), Moscow–Izhevsk: R&C Dynamics, Institute of Computer Science, 2002, pp. 296–326 (Russian).
8. Borisov, A. V. and Mamaev, I. S., Strange Attractors in Rattleback Dynamics, *Uspekhi Fiz. Nauk,* 2003, vol. 173, no. 4, pp. 408–418 [*Physics-Uspekhi,* 2003, vol. 46, no. 4, pp. 393–403].
9. Shilnikov, L. P., Bifurcation Theory and Turbulence, in *Methods of Qualitative Theory of Differential Equations,* E. A. Leontovich (Ed.), Gorky: Gorky Gos. Univ., 1986, pp. 150–165, 215 (Russian).
10. Gonchenko, S. V., Turaev, D. V., and Shilnikov, L. P., On Newhouse Domains of Two-Dimensional Diffeomorphisms That Are Close To a Diffeomorphism with a Structurally Unstable Heteroclinic Contour, in *Dynamical Systems and Related Topics: Collection of Articles to the 60th Anniversary of Academician D. V. Anosov,* Tr. Mat. Inst. Steklova, vol. 216, Moscow: Nauka, 1997, pp. 76–125 [*Proc. Steklov Inst. Math.,* 1997, vol. 216, pp. 70–118].
11. Gonchenko, S. V., Shilnikov, L. P., and Stenkin, O. V., On Newhouse Regions with Infinitely Many Stable and Unstable Invariant Tori, in *Proc. of Intern. Conf. "Progress in Nonlinear Science": Dedicated to 100th Anniversary of A. A. Andronov,* N. Novgorod, 2002, pp. 80–102.
12. Lamb, J. S. W. and Stenkin, O. V., Newhouse Regions for Reversible Systems with Infinitely Many Stable, Unstable and Elliptic Periodic Orbits, *Nonlinearity,* 2004, vol. 17, no. 4, pp. 1217–1244.
13. Delshams, A., Gonchenko, S. V., Gonchenko, A. S., Lázaro, J. T., and Sten'kin, O., Abundance of Attracting, Repelling and Elliptic Periodic Orbits in Two-Dimensional Reversible Maps, *Nonlinearity,* 2013, vol. 26, no. 1, pp. 1–33.
14. Newhouse, S. E., The Abundance of Wild Hyperbolic Sets and Non-Smooth Stable Sets for Diffeomorphisms, *Publ. Math. Inst. Hautes Études Sci.,* 1979, vol. 50, no. 1, pp. 101–151.
15. Gonchenko, S. V., Turaev, D. V., and Shilnikov, L. P., On the Existence of Newhouse Regions Near Systems with Non-Rough Poincaré Homoclinic Curve (Multidimensional Case), *Dokl. Ross. Akad. Nauk,* 1993, vol. 329, no. 4, pp. 404–407 [*Russian Acad. Sci. Dokl. Math.,* 1993, vol. 47, no. 2, pp. 268–283].
16. Palis, J. and Viana, M., High Dimension Diffeomorphisms Displaying Infinitely Many Sinks, *Ann. of Math. (2),* 1994, vol. 140, no. 1, pp. 91–136.
17. Romero, N., Persistence of Homoclinic Tangencies in Higher Dimensions, *Ergodic Theory Dynam. Systems,* 1995, vol. 15, no. 4, pp. 735–757.
18. Gonchenko, S., Shilnikov, L., and Turaev, D., Homoclinic Tangencies of Arbitrarily High Orders in Conservative and Dissipative Two-Dimensional Maps, *Nonlinearity,* 2007, vol. 20, no. 2, pp. 241–275.
19. Newhouse, S. E., Diffeomorphisms with Infinitely Many Sinks, *Topology,* 1974, vol. 13, pp. 9–18.
20. Turaev, D. V. and Shil'nikov, L. P., An Example of a Wild Strange Attractor, *Mat. Sb.,* 1998, vol. 189, no. 2, pp. 137–160 [*Sb. Math.,* 1998, vol. 189, nos. 1–2, pp. 291–314].
21. Turaev, D. V. and Shil'nikov, L. P., Pseudohyperbolicity and the Problem on Periodic Perturbations of Lorenz-Type Attractors, *Dokl. Akad. Nauk,* 2008, vol. 418, no. 1, pp. 23–27 [*Russian Dokl. Math.,* 2008, vol. 77, no. 1, pp. 17–21].
22. Gonchenko, S. V., Ovsyannikov, I. I., Simó, C., and Turaev, D., Three-Dimensional Hénon-Like Maps and Wild Lorenz-Like Attractors, *Internat. J. Bifur. Chaos Appl. Sci. Engrg.,* 2005, vol. 15, no. 11, pp. 3493–3508.
23. Gonchenko, A. S. and Gonchenko, S. V., On Existence of Lorenz-Like Attractors in a Nonholonomic Model of Celtic Stones, *Rus. J. Nonlin. Dyn.,* 2012, vol. 9, no. 1, pp. 77–89 (Russian).
24. Gonchenko, A. S., On Lorenz-Like Attractors in Model of Celtic Stone, *Vestn. Udmurtsk. Univ. Mat. Mekh. Komp. Nauki,* 2013, no. 2, pp. 3–11 (Russian).
25. Borisov, A. V. and Mamaev, I. S., *Dynamics of a Rigid Body,* Moscow–Izhevsk: R&C Dynamics, Institute of Computer Science, 2001 (Russian).
26. Borisov, A. V., Jalnine, A. Yu., Kuznetsov, S. P., Sataev, I. R., and Sedova, J. V., Dynamical Phenomena Occurring Due To Phase Volume Compression in Nonholonomic Model of the Rattleback, *Regul. Chaotic Dyn.,* 2012, vol. 17, no. 6, pp. 512–532.
27. Karapetyan, A. V., Hopf Bifurcation in a Problem of Rigid Body Moving on a Rough Plane, *Izv. Akad. Nauk SSSR. Mekh. Tverd. Tela,* 1985, no. 2, pp. 19–24 (Russian).
28. Shilnikov, L. P., Existence of a Countable Set of Periodic Motions in a Neighborhood of a Homoclinic Curve, *Dokl. Akad. Nauk SSSR,* 1967, vol. 172, no. 2, pp. 298–301 (Russian).
29. Anishchenko, V. S., *Complicated Oscillations in Simple Systems,* Moscow: Nauka, 1990 (Russian).
30. Vitolo, R., Bifurcations of Attractors in 3D Diffeomorphisms, *PhD Thesis,* Groningen Univ. Press, 2003.
31. Shilnikov, L. P., The Bifurcation Theory and the Lorenz Model, in *Bifurcation of the Cycle and Its Applications,* Moscow: Mir, 1980, pp. 317–335 (Russian).
32. Gonchenko, A. S., Gonchenko, S. V., and Kazakov, A. O., On Some New Aspects of Celtic Stone Chaotic Dynamics, *Rus. J. Nonlin. Dyn.,* 2012, vol. 8, no. 3, pp. 507–518 (Russian).

33. Kuznetsov, S. P., Jalnine, A. Y., Sataev, I. R., and Sedova, J. V., Phenomena of Nonlinear Dynamics of Dissipative Systems in Nonholonomic Mechanics of the Rattleback, *Rus. J. Nonlin. Dyn.,* 2012, vol. 8, no. 4, pp. 735–762 (Russian).
34. Gonchenko, A. S., Gonchenko, S. V., and Shilnikov, L. P., Towards Scenarios of Chaos Appearance in Three-Dimensional Maps, *Rus. J. Nonlin. Dyn.,* 2012, vol. 8, no. 1, pp. 3–28 (Russian).
35. Anosov, D. V., Geodesic Flows on Closed Riemannian Manifolds of Negative Curvature, *Trudy Mat. Inst. Steklov,* 1967, vol. 90, pp. 3–209 [*Proc. Steklov. Inst. Math.,* Providence, R. I.: AMS, 1969].
36. Afraimovich, V. S. and Shil'nikov, L. P., Strange Attractors and Quasiattractors, in *Nonlinear Dynamics and Turbulence,* G. I. Barenblatt, G. Iooss, D. D. Joseph (Eds.), Interaction Mech. Math. Ser., Boston, MA: Pitman, 1983, pp. 1–34.
37. Anosov, D. V. and Solodov, V. V., Hyperbolic Sets, in *Dynamical Systems – 9,* Encyclopaedia Math. Sci., vol. 66, Berlin: Springer, 1995, pp 10–92.
38. Afraimovich, V. S., Bykov, V. V., and Shil'nikov, L. P., On Attracting Structurally Unstable Limit Sets of Lorenz Attractor Type, *Trudy Moskov. Mat. Obshch.,* 1982, vol. 44, pp. 150–212 [*Trans. Mosc. Math. Soc.,* 1982, vol. 44, pp. 153–216].
39. Ruelle, D., Small Random Perturbations of Dynamical Systems and the Definition of Attractors, *Comm. Math. Phys.,* 1981, vol. 82, pp. 137–151.
40. Auslander, J. and Seibert, P., Prolongations and Stability in Dynamical Systems, *Ann. Inst. Fourier (Grenoble),* 1964, vol. 14, fasc. 2, pp. 237–267.
41. Gonchenko, A. S., Gonchenko, S. V., Ovsyannikov, I. I., and Turaev, D., Lorenz-Like Attractors in Three-Dimensional Hénon Maps, *Math. Model. Nat. Phenom.,* 2013, Vol. 8, No. 5, pp. 80–92.
42. Afraimovich, V. S. and Shil'nikov, L. P., On invariant two-dimensional tori, their breakdown and stochasticity, *Methods of the Qualitative Theory of Differential Equations (Gorky),* 1983, pp. 2–26. [English translation in: Amer. Math. Soc. Transl., 149 (1991), pp. 201–212].